International Journal of High-Rise Buildings
December 2015, Vol 4, No 4, 271-281

International Journal of
High-Rise Buildings
www.ctbuh-korea.org/ijhrb/index.php

Numerical Analysis for High-rise Building Foundation and Further Investigations on Piled Raft Design

Jinoh Won[1], Jin Hyung Lee[2], and Chunwhan Cho[1,†]

[1]*Deputy General Manager, Technical Advisory Team, Samsung C&T, Seoul, Korea*
[2]*Manager, Technology Development Team, Samsung C&T, Seoul, Korea*

Abstract

This paper introduces detailed three-dimensional numerical analyses on a bored pile foundation for a high-rise building. A static load test was performed on a test pile and a numerical model of a single pile, which was calibrated by comparing it with the test result. The detailed numerical analysis was then conducted on the entire high-rise building foundation. Further study focused on soil pressures under the base slab of a piled raft foundation. Total seven cases with different pile numbers and raft-soil contact conditions were investigated. The design criteria of a foundation, especially settlement requirement were satisfied even for the cases with fewer piles under considerable soil pressure beneath the base slab. The bending moment for the structural design of the base slab was reduced by incorporating soil pressures beneath the base slab along with bored piles. Through the comparative studies, it was found that a more efficient design can be achieved by considering the soil pressure beneath the slab.

Keywords: Pile foundation, Piled raft, Numerical model

1. Introduction

In the design of foundation for a high-rise building, it is important to integrate all information from ground conditions and structural loadings including its uncertainty and other unknown hidden risks. Sufficient soil investigation can reduce the risk of failure or excessive settlement of building foundations, which can result in a safer design. It is important to note that even a small defect or a certain differential settlement can bring to significant impact on the entire superstructure especially for high-rise building. After failure, immeasurable repair cost and time delay will be followed as consequences. Therefore, it is common that a high-rise building foundation is designed with enough safety margins and individual pile bearing capacities, which is to be validated at sites by carrying out the loading tests.

Many analytical and numerical solutions have been developed in several decades for the analysis of piled-raft foundation system (Poulos, 1991; Butterfield & Banerjee, 1971; Hain & Lee, 1978, Ta & Small, 1996; Zhuang et al., 1991; Katzenbach et al., 1998a, 1998b). The design philosophy of a piled-raft system was summarized by Poulos (2001, Poulos). Yet, many designers so far have hesitated to use the piled raft design philosophy for a high-rise building not only because the design methods of a piled raft system are not easy to use and carry many uncertainties on the numerical modeling but because designers are also willing to use the raft resistance as a margin of safety in their foundation design.

The high-rise building foundation design introduced here was also designed by incorporating pile group analysis concept without considering raft resistance. In this traditional method, only piles beneath the base slab resist the whole superstructure loadings, and the ground is assumed to be separated from the base slab. In this paper, further studies apply a three-dimensional numerical tool to investigate the influence of raft resistance on the behavior of a building foundation which consists of bored piles and a base slab. The results of these numerical comparative studies based on actual cases may enhance our understanding of a piled raft system and provide useful information for the more optimized foundation design of high-rise buildings.

2. Soil Investigation and Pile Load Test

2.1. Soil investigation

The high-rise building located in South East Asia consists of a 48-stories tower and a 5-stories basement. The size of building base is about 64 m × 39 m and the depth of basement bottom is 21 m. The bored piles are used for supporting the building. The excavation depth of the bored piles are approximately 78.0 m of which effective length is about 57 m and the diameters are 1.2 m, 1.5 m and 1.8 m depending on column axial loads. The total number of

†Corresponding author: Chunwhan Cho
Tel: +82-2-2145-6854; Fax: +82-2-2145-6581
E-mail: chunwhan.cho@samsung.com

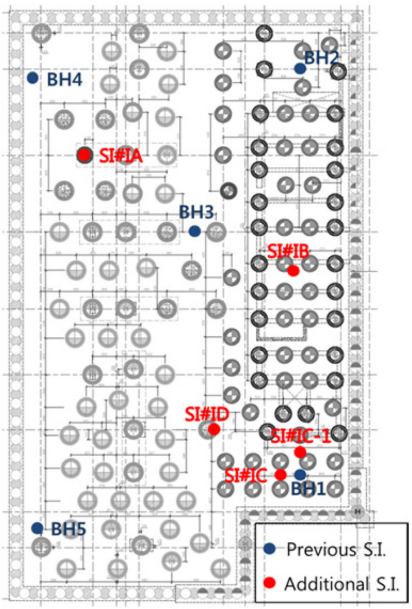


Figure 1. Boring hole locations.

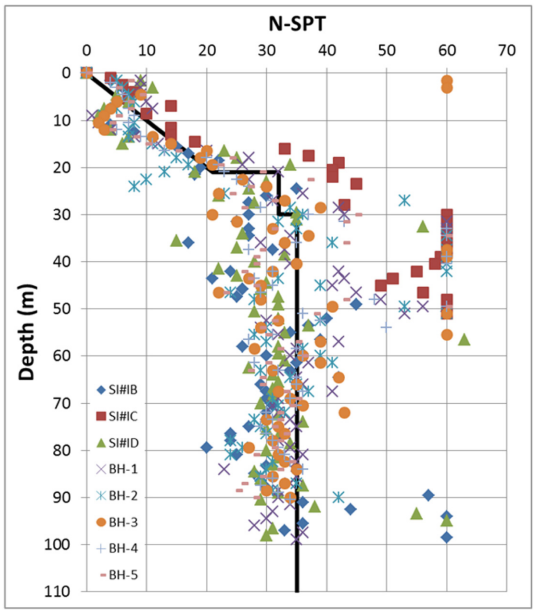


Figure 2. SPT-N values with depth.

piles is 134.

The ground conditions were investigated twice for this project. In the first soil investigation, five bore holes, BH 1~ BH 5, were drilled and tested for the early stage of foundation design. The number of bore holes was not sufficient and some laboratory test results were not matched well with each other, making it difficult to be used for a detail foundation design. Therefore, additional soil investigation was planned and carried out: total four boreholes, SI #1A ~ #1D, were added to the previous five boreholes. Additional laboratory tests were also carried out to estimate accurate soil properties. Fig. 1 shows the plan view of the soil investigation locations at the project site. Table 1 and Table 2 show the soil properties for the numerical analysis which were estimated at the preliminary stage and at the detailed design stage, respectively. As shown in the tables, the elastic modulus and undrained shear strength values for the second investigation in general are smaller than from the first investigation. One may criticize the increase in foundation size by using lower values of soil properties after carrying out additional soil investigation. However, it is important to remember that accurate soil properties are obtained through additional soil investigations, which provide a more accurate and reliable design,

Table 1. Soil properties at the first investigation

Layer	Layer 1-1	Layer 1-2	Layer 2	Layer 3
Depth (m)	0~15	15~21	21~30	30~
Drainage	Undrained	Undrained	Undrained	Undrained
γ_{sat} (kN/m^3)	15.5	14.2	14.2	18.1
E (kN/m^2)	14,400	78,000	115,000	115,000
n	0.49	0.49	0.49	0.49
c_u (kN/m^2)	36	138	210	204
ϕ (°)	0	0	0	0

Table 2. Soil properties at the second investigation

Layer	Layer 1	Layer 2	Layer 3
Depth (m)	0~21	21~30	30~
Drainage	Undrained	Undrained	Undrained
γ_{sat} (kN/m^3)	16.0	16.0	18.0
E (kN/m^2)	0~42,000	64,000	70,000
n	0.49	0.49	0.49
c_u (kN/m^2)	0~126	192	210
ϕ (°)	0	0	0

reduce risks of losing time in the long run, and build hedges against foundation failure risks.

Fig. 2 shows SPT-N values up to maximum 100 m depth. The design pile cut-off level is GL.-21.0 m. The top soil above pile cut-off level is sandy silt or clayey silt. It is followed by stiff clayey silt and stiff silty clay at GL.-21 m up to GL.-30 m of which SPT-N values are 30~35. Shallow thickness of sand layer exists at depth of 30 m to 33 m and is followed by very thick stiff clay layer up to 90 m. The SPT-N values for sand layer and stiff clay layer ranges 20~60, but the average value used for design is about 30. As shown in the Fig. 2, there are no firm founding layers for end-bearing of piles so that the estimation of appropriate pile lengths and settlement predictions were outstanding issues at the design stage. The pile load tests were performed to confirm those issues at the site at the design stage.

2.2. Pile load test and its numerical modeling

2.2.1. Preparation of pile load test

Fig. 3 shows the test pile location and a schematic diagram of pile loading system. The test pile is a working pile with 1.8 m diameter with effective length of 56.8 m. Pile toe level is GL. -77.8 m. The bored pile was equipped with total 56 strain gauges, a vibrating wire strain type, to investigate detailed load transfer behavior of shaft and pile toe. Two tell-tale extensometers were installed not only at cut-off level of the test pile but also at the pile toe to measure pile settlement at both depths. The magnitude of applied loads was measured using four vibrating wire load cells (VWLC) installed above the hydraulic jack. The pile settlement was also monitored independently by measuring levels of the target attached on the pile surface during load tests, and it was compared with the settlements measured by tell-tale extensometers. In addition, four dial gauges were installed at the top of the test pile, and single dial gauges were installed at the top of each reaction pile to estimate settlement and extension of test and reaction piles, respectively.

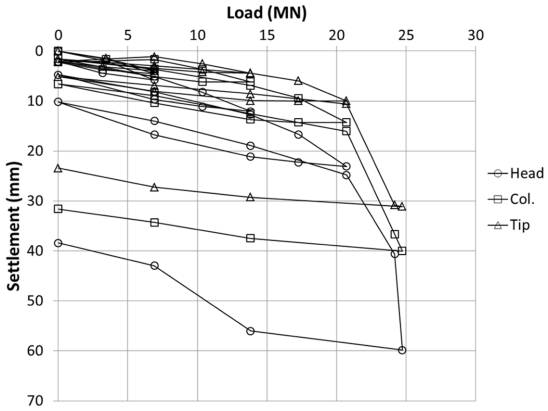
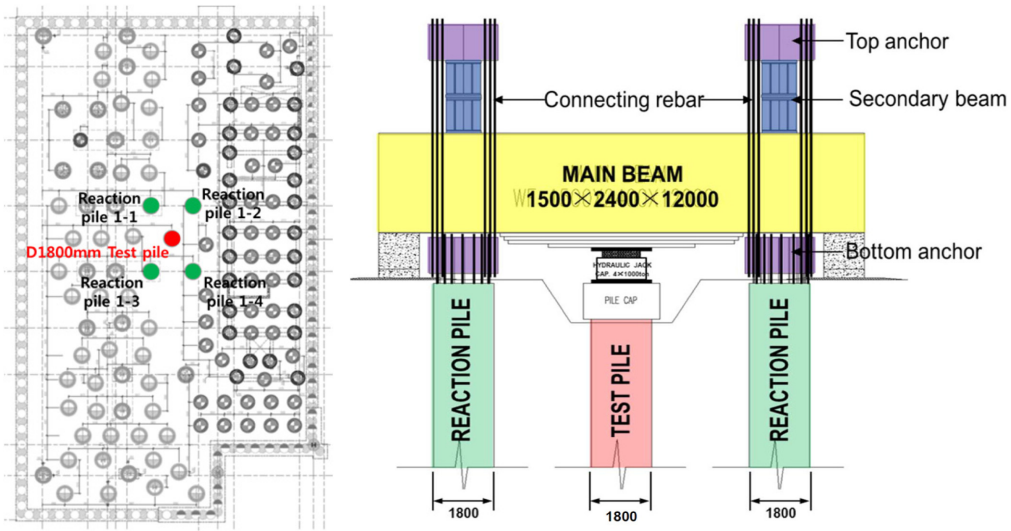


Figure 4. Load-settlement relationship at pile head.

The axial loading was applied on the test piles by the reaction pile system as shown in Fig. 3. The test was performed in accordance with ASTM D1134-07. The working load (WL) of the test pile was 14.1 MN and four loading cycle was scheduled: 7.1 MN (0.5WL), 14.1 MN (1WL), 21.2 MN (1.5WL) and 28.2 MN (2WL).

2.2.2. Test results

Fig. 4 shows the load-settlement curves at pile head, cut-off-level (col) and pile toe level. The test was terminated at fourth cycle with maximum load 25.2 MN (1.78 WL) due to occurrence of excessive settlement. Pile settlement



(a) Layout (b) Loading System

Figure 3. Static load test of reaction pile system.

Table 3. Results of allowable bearing capacity (Qa) of the pile

Analysis methods	Qa (kN) Dial gauge	Qa (kN) Survey	Remark (General comments from the reference)
Davisson	11,907	11,466	Under-estimate
Chin	15,798	14,847	Over-estimate
Mazurkiewicz	13,054	12,377	Good relation for plunging failure
S-logT	12,093	12,093	
DIN4026	12,397	11,956	Conservative estimate
Average	12,515	12,142	

*Factor of Safety: 2.0
*Average value was calculated except the maximum and the minimum values.

Table 4. Result of pile head settlement

Load (MN)	Total settlement (mm)	Net settlement (mm)	Remarks
100% WL (14.1)	12.08	4.74	25 mm (Allowable settlement)

Table 5. Back-calculated maximum unit shaft resistance and maximum end-bearing resistance

Elev. Below ground surface (m)	Max. unit skin friction (kN/m^2)
-8.2~-16.9	57.8
-16.9~-19.9	90.2
-19.9~-24.0	61.7
-24.0~-30.0	51.9
-30.0~-35.0	34.3
-35.0~-40.0	76.4
-40.0~-45.0	72.5
-45.0~-50.0	71.5
-50.0~-54.0	63.7
-54.0~-58.0	66.6
-58.0~-62.0	63.7
-62.0~-64.5	39.2
End-bearing (kN)	3,949.4

Table 6. Design parameters of bored pile and raft

Parameter	Bored pile	Raft
Young's modulus (E) (GN/m^2)	25.7	25.7
Unit weight (γ) (kN/m^3)	25	25
Diameter / thickness (m)	1.8 / 1.5	3.0
Poisson's ratio (ν)	0.2	0.2

was measured by both dial gauges and target surveys. The ultimate bearing capacity and allowable bearing capacity were estimated using several methods: 1) Davisson, 2) Chin, 3) Mazurkiewicz, 4) S-logT and 5) DIN4026. The allowable bearing capacities interpreted by different methods are summarized in Table 3. The average value is about 12.4 MN. Table 4 shows the pile head settlement at the service load. Based on the pile load tests, maximum unit shaft resistance and end-bearing resistance are estimated as shown in Table 5. Through these load test results, the each pile design load was evaluated and additional piles were added to the original pile layout.

2.2.3. Validation of single pile numerical model

The validity of the 3D FE model was examined by comparing its result with the result of a static load test. Fig. 5 shows a 3D FE model used for an axially loaded single

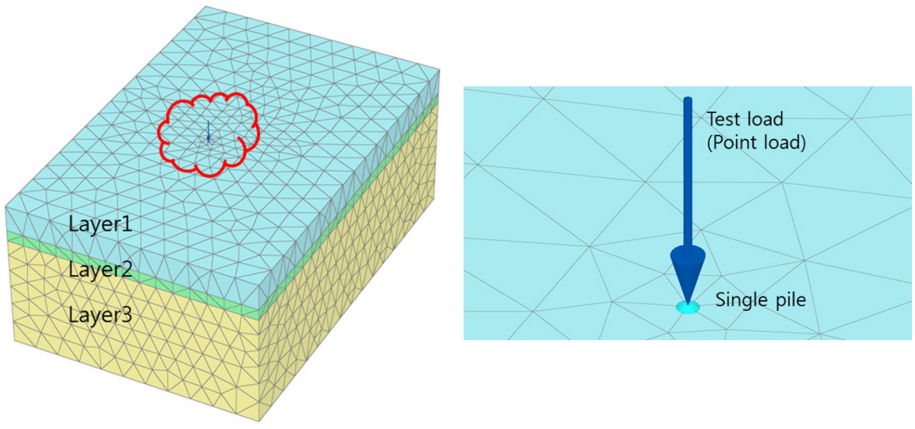


Figure 5. 3D FE model of single pile.

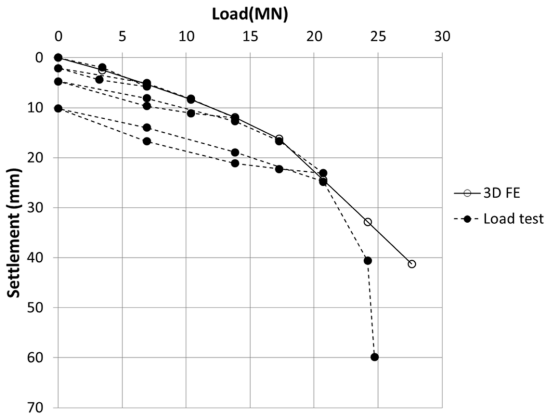


Figure 6. Comparison between static load test and 3D FE analysis result.

pile. Soil volume surrounding a pile was modeled using 10-node tetrahedral elements in PLAXIS Program and a Mohr-Coulomb model for representing non-linear soil behavior. An embedded pile element in PLAXIS was used for pile modelling, in which shaft and end-bearing resistance of pile derived from the single pile load test were used as shown in Table 5. The pile was assumed to be in a stress-free state at the initial equilibrium stage without considering pile installation effect. Elastic model was used

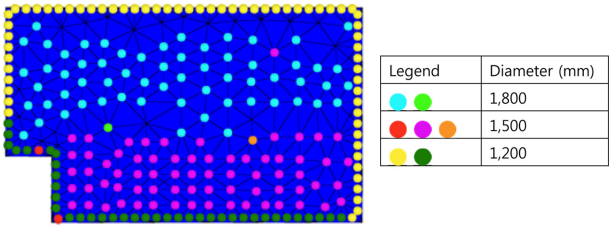


Figure 7. Foundation section and pile layout.

for the piles and the raft slab. Their structural parameters are shown in Table 6.

Fig. 6 shows predicted settlements of the 3D FE analysis with measured settlements of static load test. The figure shows how 3D FE analysis executed reasonably close pile head settlement result to the measured along the loading steps from 0 to 150%. However, the prediction did not match fully with result measured at over 150% loading. It appears that there is limitation in using characterized numerical model for representing the actual nonlinearity and sudden yielding of the pile-soil, which interact at about 178% of loading stage. Though some discrepancies appear at the ultimate stage, the current single pile model appears insignificant to represent behavior of pile foundations under the working loads of the building.

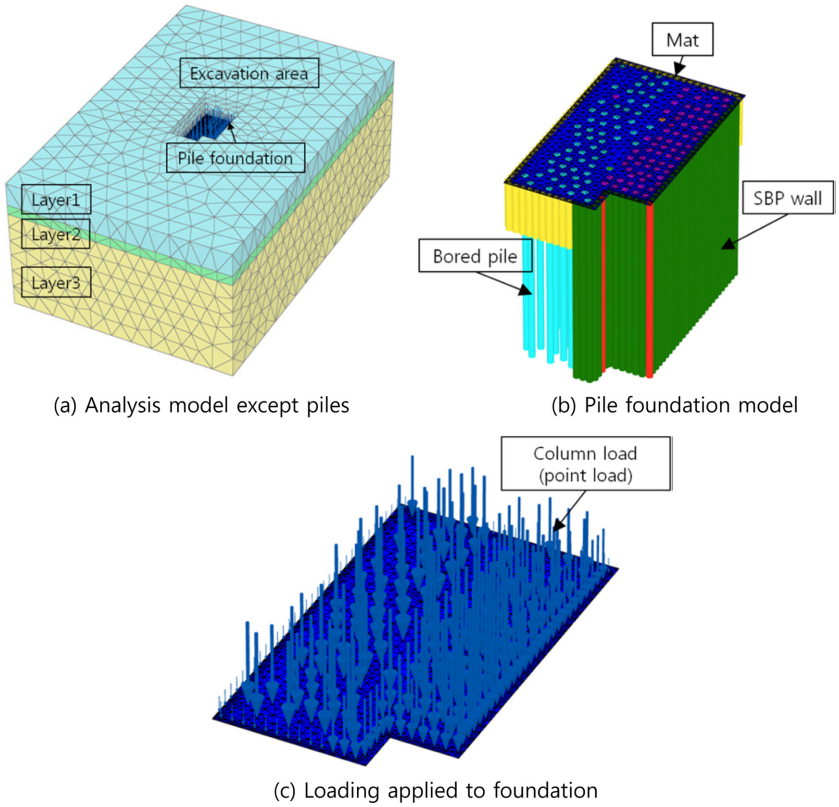


Figure 8. Typical analysis model.

3. Numerical Analysis for Building Foundation

3D FE analysis was performed to estimate the settlement of the entire building foundation beneath the proposed permanent total loading. The base slab of the building is an almost rectangular shape of approximately 64 m long by 39 m wide with 3 m thickness. For bored piles, typical pile length is 56.8 m with a diameter of 1.8 m or 1.5 m; the total number of piles is 134. The length of SBP (Secant Bored Pile) wall is 15 m and 57 m with a diameter of 1.2 m, 1.5 m, respectively; the total number of SBP wall piles is 102. Fig. 7 shows the layout of the bored piles and SBP wall. The total loading of the entire building was 1,636 MN. As shown in Fig. 8, the raft was modeled as plate elements and each pile under the raft was rigidly connected to the plate element. The soil and structural properties are shown in Table 2 and Table 6, respectively. The whole mesh was used for these 3D analyses due to asymmetric shape of raft and pile layout. The boundary condition for each pile was same with the single pile case. For the prediction of real raft settlement, the modeled raft contacted with the element of ground.

Fig. 9 shows the settlement profile of the building foundation. The maximum settlement is 112 mm and the minimum settlement is 36 mm.

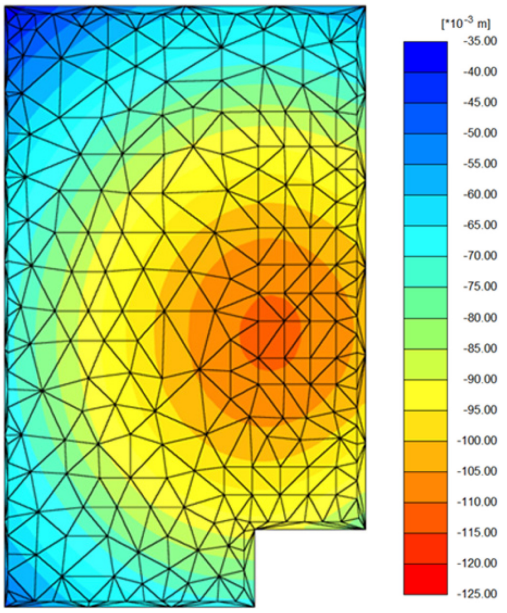


Figure 9. Settlement profile at the building foundation (Uz max = 0.112 m, Uz min = 0.036 m).

4. Further Numerical Studies from the Piled Raft Foundation Viewpoint

4.1. Case analysis

Further studies focused on the investigation of the two factors: 1) pile numbers and arrangements, and 2) effect of raft-soil contact. Total seven compared cases are shown in Table 7. Fig. 10 shows original pile layout and two other pile arrangements that have smaller number of piles than the original. Three cases, i.e., case 4~6, represent pile group cases, in which the raft was separated from underlying ground, but pile arrangements were the same with the piled raft cases (case 1~3). A raft-only case (case 7) without piles was analyzed to compare with piled foundations. The result provided reference values for the settlements and bending moments of foundation to the piled raft and pile group cases. All cases were analyzed based on the construction sequences as follows: a) initial condition, b) installation of bored piles and retaining wall, c) excavation, d) raft casting, and e) loads application.

4.2. Analysis results

4.2.1. Settlement

Figs. 11 and 12 show the settlement of raft slab for piled raft and pile groups at the working load, respectively. The results shows that general shapes of settlement profile are similar with each other even when settlement has increased while pile number has decreased. However, a raft-only case (case 7) showed different settlement profile as shown in Fig. 13. Unlike other cases, the maximum settlement of case 7 occurred near the right-side wall, and its values were also larger than other pile foundation cases. Fig. 14 shows the load vs. settlement curve for raft-only case. At the working load, extremely large settlement of 277.1 mm occurred near the right-side wall, and 550 mm settlement occurred when 150% of working load was applied. Therefore, it is appropriate to assert that pile foundation was necessary in constructing this building in order to reduce exessive settlement.

Maximum settlement and rotation for all cases are summarized in Table 9. In this study, Chinese standard was adopted for defining settlement criteria for buildings. The allowable settlement adopted in this study was 200 mm and allowable rotation was 1/500 considering the size and the shape of this building. The maximum settlement for

Table 7. Case analysis

	Pile arrangement case (pile number)		
	Original	Pile omit (version 1)	Pile omit (version 2)
Piled raft (contacted)	Case 1 (134ea)	Case 2 (112ea)	Case 3 (81ea)
Pile groups (un-contacted)	Case 4 (134ea)	Case 5 (112ea)	Case 6 (81ea)
Raft only		Case 7	

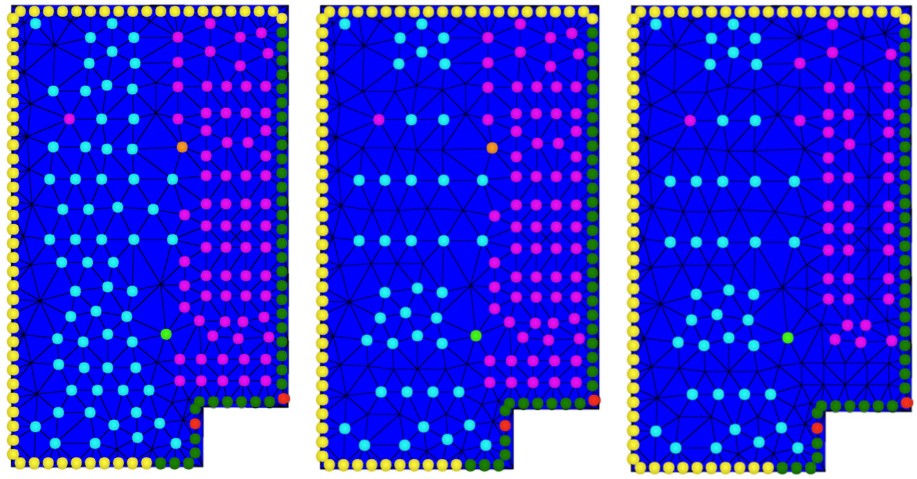


Figure 10. Pile arrangements.

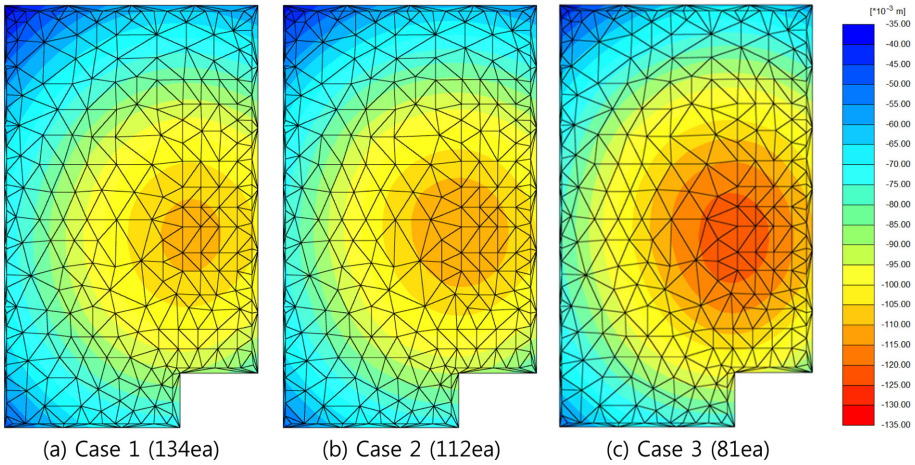


Figure 11. Settlement profile for the piled raft.

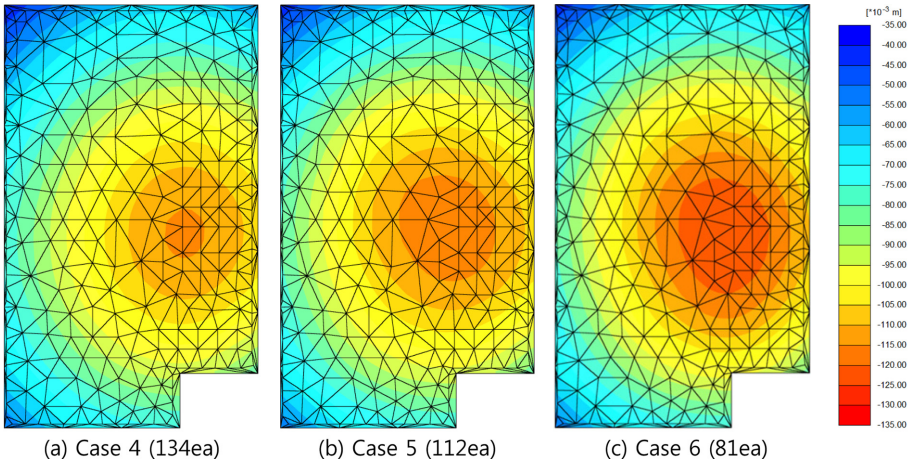


Figure 12. Settlement profile for the pile group.

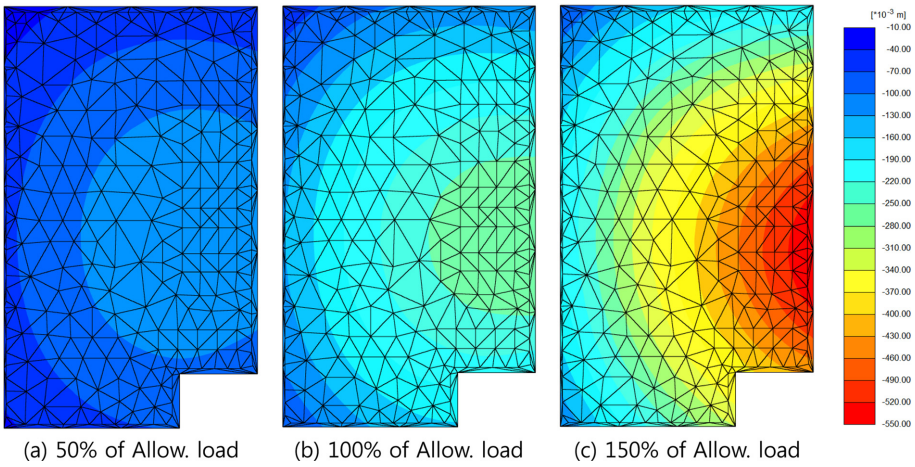


Figure 13. Settlement profile for the raft only.

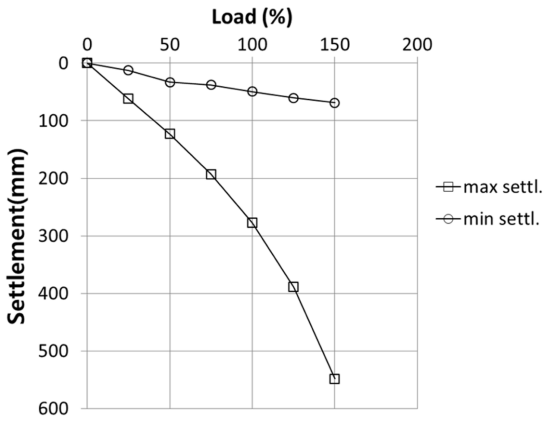


Figure 14. Load settlement curves for raft-only case (case 7).

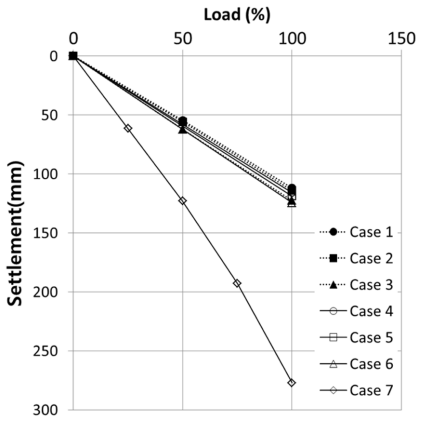


Figure 15. Load settlement curves for piled rafts with raft-only case.

Table 9. Summary of the settlement of the analysis

	Piled raft			Pile groups			Raft
	Case 1	Case 2	Case 3	Case 4	Case 5	Case 6	Case 7
Max. settlement (mm)	111.7	113.9	122.6	115.8	118.7	124.6	277.1
Min. settlement (mm)	36.5	37.6	39.9	40.1	41.0	40.7	43.9
Max. rotation	0.0016	0.0018	0.0018	0.0017	0.0019	0.0019	0.0044
Comments	Ok	Ok	Ok	Ok	Ok	Ok	N.G
Reference	Allowable settlement = 200 mm, Allowable rotation = 0.002 (1/500)						

case 1 was 111.7 mm and its maximum rotation was 0.0016. Both met the requirement of settlement and rotation applied in this study. The number of piles for case 3 was about 60% of case 1. Yet, the increment of settlement for case 3 compared to case 1 was only 9.7%. The settlement was still within the allowable settlement. The tendency of small increase in settlement is shown more elaborately in Fig. 15.

As shown in Fig. 15, the total settlement and differential settlement of case 1~3 (piled raft) was slightly smaller than those of case 4~6 (pile groups). This means that piled raft is more efficient than pile group for reducing base slab settlement.

4.2.2. Pile and raft load distribution

The determination of load sharing ratio between pile and raft, which is the total pile load divided by total structural load, is an important factor in design of piled raft.

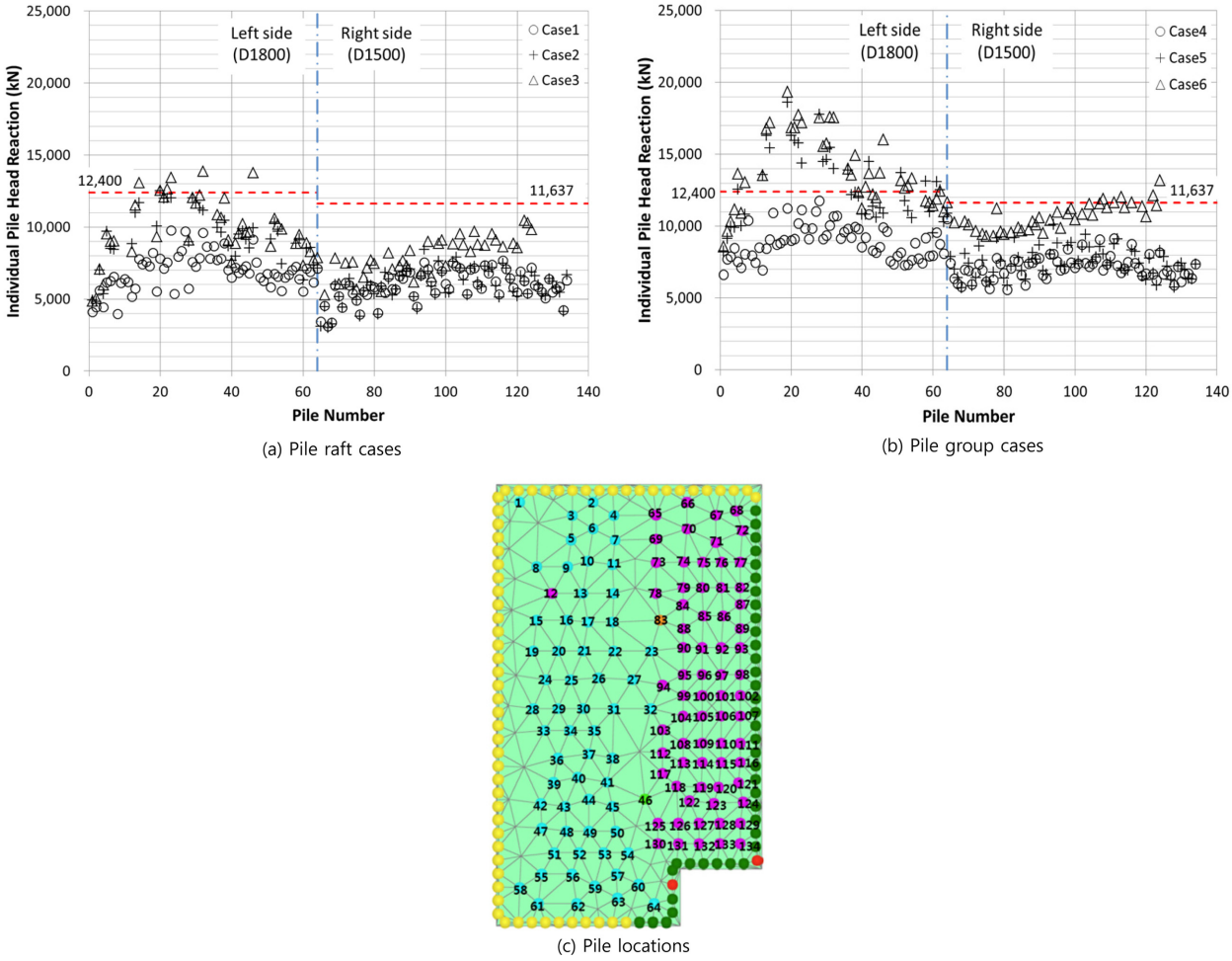
Table 10. Load-sharing ratio

	Case 1	Case 2	Case 3
Load sharing ratio (Σ(pile load) / Σ(structural load))	75 %	72 %	69 %

However, it is difficult to make an accurate prediction because load-sharing ratio can be estimated based on complex soil-pile-raft interactions. Factors that affect complex soil-pile-raft interaction are pile arrangement, individual pile's size, raft dimension and its reinforcement, strength of ground beneath base slab, and characteristics and magnitude of loading, etc. For these reasons, full three-dimensional numerical analysis method functions as the best tool to estimate such load-sharing ratio. The load-sharing ratio was estimated at three piled raft cases and summarized in Table 10. One quarter of total load was supported by soils beneath case 1 raft slab. The portion of soil pressure under the raft slab increased from 25% to 31% while the pile number decreased. As noted above, in Table 9, the maximum settlement of the raft was 111.7 mm and 122.6 mm for case 1 and case 3, respectively. At decrease in number of piles, there was increase in the maximum settlement by 10.9 mm and the load-sharing ratio of soils beneath raft slab also increased by 6% when it compared to case 1.

4.2.3. Individual pile head reaction

Main focus of piled raft design has been put on load-sharing ratio and raft settlement. However, change in individual pile head reaction from pile number should be verified because these reaction forces are used as design pile capacity. Fig. 16 shows individual pile head reactions of all piles for piled raft (case 1~3) and piled groups (case 4~6); also, each pile location was marked. In general, individual pile head reactions for piled raft are smaller than those for pile groups. The difference came from load-sharing of the raft slab for piled raft cases. The amount of loads supported by raft slab for the piled raft analyses added to individual pile reactions for the pile group ana-



(a) Pile raft cases

(b) Pile group cases

(c) Pile locations

Figure 16. Individual pile head reaction.

lyses. The allowable pile capacities used in the design were 13.2 MN and 11.6 MN for the left side (1,800 mm diameter) and the right side (1,500 mm diameter), respectively. As shown in Fig. 16, individual pile head reactions for case 3 met allowable bearing capacity in the piled raft analyses. Therefore, it was found that pile numbers could be reduced when piled raft concept was applied.

4.2.4. Bending moment at the raft slab

As mentioned earlier, a change in pile layout affected individual pile loadings and piled raft's settlement. However, there is possibility that a change in pile layout can also affect raft slab design as well, especially on the thickness of raft slab and amount of reinforcements. For such reason, change of raft slab should be noted in considering optimized pile arrangement in the piled raft design.

Fig. 17 shows bending moment profiles at two typical sections of raft for three piled raft cases along with raft-only case. It should be noted that the real raft slab was more complicated than the current model since the existence of several pits but maximum bending moment at typical sections considered in this study was not different much from the actual value. The maximum bending moment of the raft slab for case 1 was 10.8 MN-m/m. The raft slab was designed based on BS8110-97 and its concrete strength was 45 N/mm^2 and the yield strength of reinforcement was 400 N/mm^2. The typical slab thickness was 3.0 m and typical reinforcement design is 6D32-250 (six main 32 mm reinforcements per 250 mm spacing). The calculated bending moment capacity of the raft slab was 17.8 MN-m/m, which is larger than the maximum bending moment. As shown in Fig. 17, bending moment increased slightly while pile number decreased; yet the increment was not significant. The maximum bending moment for case 3 was 11.2 MN-m/m, which is still less than the bending moment capacity of the current raft slab. This means that pile number can be reduced without change of the current raft slab design. Of course, the maximum bending moment can increase significantly in local area if pile locations are not well arranged with consideration of structural loadings. From such result, it is certain that pile numbers can be reduced without increasing raft slab sizes when pile layout is well organized considering its structural loadings.

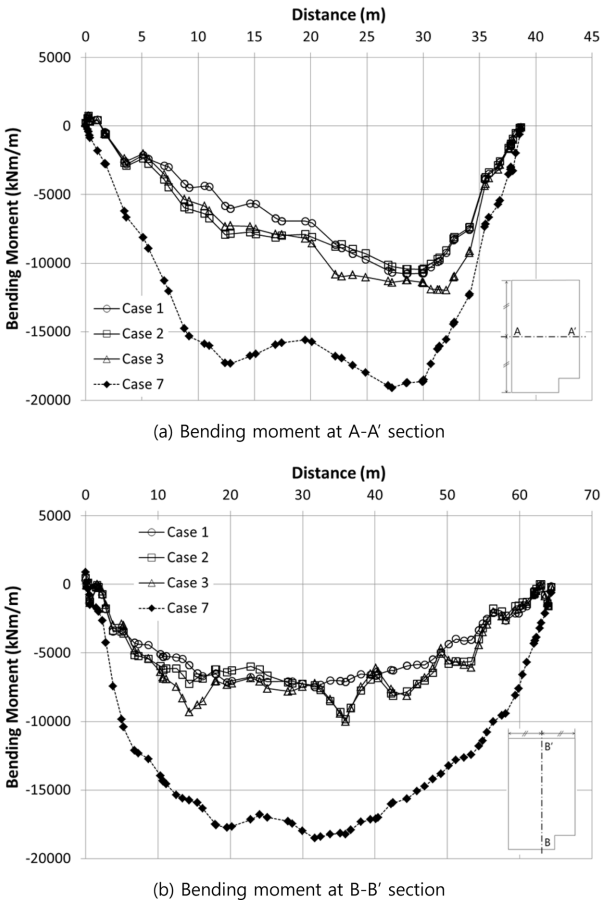


Figure 17. Bending moments at foundation slab.

As shown in Fig. 17, the raft-only case (case 7) had significantly large bending moments compared to other cases. Its maximum value was 19.1 MN-m/m. For this reason, thicker concrete slab and larger amount of reinforcement are required to resist larger bending moment for the raft-only case. Designer should consider such change in raft slab design when piles are removed for the purpose of saving piling construction cost. Under such conditions, the raft-only case is not applicable because of excessive settlement of raft slab as well as excessive bending moments at the base slab. Therefore, piles are needed to control the settlement to meet the allowable settlement of 200 mm and to reduce the bending moment of base slab.

Fig. 18 shows comparison of bending moment of the piled raft cases versus that of pile group cases. In general, bending moment of raft slab in piled raft was similar to that in pile groups. Yet, the bending moment in pile groups were slightly larger than in piled raft when pile number was smaller.

5. Summary and Conclusion

In this analysis, two design concepts on pile foundations for high-rise buildings were investigated. One is a design concept of a pile group, and the other is on a piled raft. Initially, a case study on an actual design was introduced to explain typical design process for a high-rise building foundation. Through executions of load tests and comparison between results from numerical models, greater confidence was achieved on a pile design. The numerical model, which utilized back-calculated pile-soil interaction parameters, provided realistic behavior of the building foundation. Also, further study was focused on the effect of raft-soil contact and pile arrangement in piled raft design.

The conclusions from these numerical studies are as

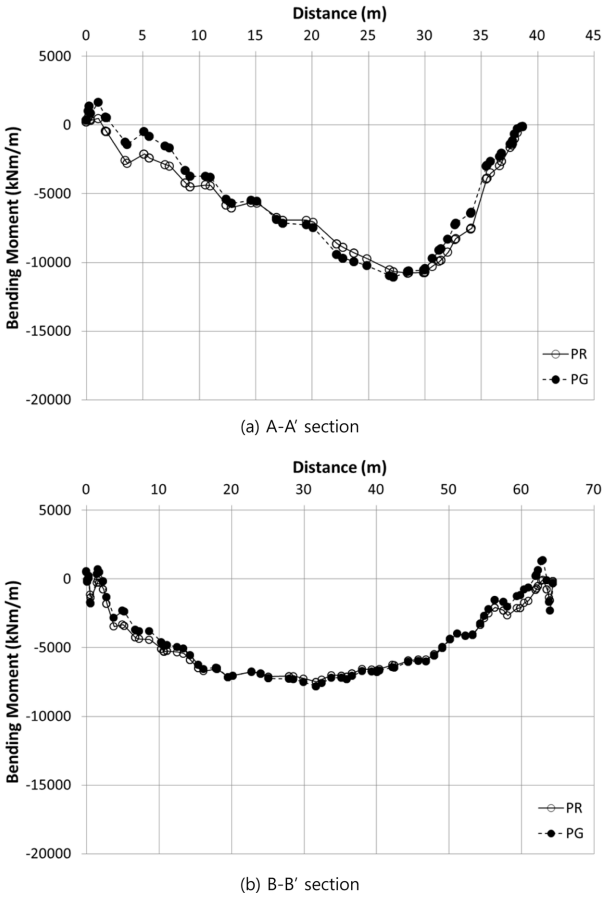


Figure 18. Bending moment comparison between piled raft vs. pile groups (case 1 vs. case 4).

follows:

(1) The raft-only case is not applicable to this building due to excessive settlement and bending moment of the base slab.

(2) The current pile foundation, which has been designed using a pile group concept, had enough margins to achieve the settlement criteria. Thus, approximately 60% of its pile number met the settlement criteria.

(3) In pile group analyses, individual pile head reaction exceeded the allowable bearing capacities while pile number decreased. However, pile head reactions from piled raft analyses for the same pile arrangement were smaller than those for pile groups; so that even 60% of pile number cases have satisfied the requirement of allowable bearing capacities of individual piles.

(4) The bending moment of raft slab increased as pile number decreased while the increment was not significant. Pile number could be reduced without increasing raft slab sizes if pile layout was well organized considering its structural loadings.

References

Butterfield, R. and Banerjee, P. K. (1971). "The elastic analysis of compressible piles and pile groups." *Geotechnique*, 21(1), pp. 43~60.

Hain, S. J. and Lee, I. K. (1978). "The analysis of flexible raft-pile systems," *Geotechnique*, 28(1), pp. 65~83.

Ta, L. D. and Small, J. C. (1996). "Analysis of piled raft systems in layered soils." *International Journal for Numerical and Analytical Methods in Geomechanics*, London, 20(1), pp. 57~72.

Katzenbach, R., Arslan, U., and Moormann, C. (1998a). "Design and safety concept for piled raft foundations." Proc. 3th International Geotechnical Seminar on Deep Foundation on Bored and Auger Piles, Ghent, Balkema, Rotterdam, pp. 439~448.

Katzenbach, R., Arslan, U., Moorman, C., and Reul, O. (1998b). "Piled raft foundation- Interaction between piles and raft," International Conference on Soil-Structure Interaction in Urban Civil Engineering, Darmstadt, 8-9, October, vol. 2, No. 4, pp. 279~296.

Poulos, H. G. (1991). "Analysis of piled strip foundations." Proc. of Conference on computer methods and advances in geomechanics, Rotterdam: Balkema, pp. 183~191.

Poulos, H. G. (2001). "Piled-raft foundations; design and applications." *Geotechnique*, 51(2), pp. 95~113.

Zhuang, G. M., Lee, I. K., and Zhao, X. H. (1991). "Interactive analysis of behaviour of raft-pile foundations." Proc. of Geo-Coast '91, Yokohama 2, pp. 759~764.